Development of Silica-Copper Nanocomposite for Water Purification

Sajeevan Angappan[1], Mudith Karunaratne[2], Charitha Thambiliyagodage[3]

[1] Department of Materials Engineering, Faculty of Engineering, Sri Lanka Institute of Information Technology, Malabe, Colombo, Sri Lanka.
[2] Department of Materials Engineering, Faculty of Engineering, Sri Lanka Institute of Information Technology, Malabe, Colombo, Sri Lanka.
[3] School of Science and Education, Faculty of Humanities and Sciences, Sri Lanka Institute of Information Technology, Malabe, Colombo, Sri Lanka.
[1] sajeevanangappan@gmail.com, [2] mudith.k@sliit.lk, [3] charitha.t@sliit.lk

Leshan Usgodaarachchi[4]
[4] Department of Materials Engineering, Faculty of Engineering, Sri Lanka Institute of Information Technology, Malabe, Colombo, Sri Lanka.
[4] leshan.u@sliit.lk

ABSTRACT

Water pollution is one of the serious concerns across the world at the moment. Industrial wastewater significantly contributes to the negative impacts caused by water pollution. Textile industries discharge large amounts of effluents into water streams with little or no treatment of the discharge because wastewater treatment is an expensive process. Thus, there exists a need for a cheap and effective way to treat textile effluent that contains dyes before being discharged. A high purity silica-based Nano-adsorbent was synthesized by using rice husk as the commercially available main cheap precursor. Copper-loaded silica nanoparticles were successfully functionalized with 3-aminopropyl triethoxysilane (APTES) via the sol-gel pathway to enhance the adsorption performance of organic dyes from textile effluent. The performance of produced Nano-adsorbent was evaluated by using methylene blue as waste adsorbate. As synthesized nanomaterial was characterized by X-Ray Diffraction (XRD) and Fourier Transform Infrared (FTIR) spectroscopy, the XRD results confirmed the presence of silicon dioxide (SiO_2) and paramelaconite (Cu_4O_3) as predicted. The FTIR confirmed the presence of Si–O stretching, N-H bending, C–H stretching, Cu–O stretching and O–H bending vibrations thereby suggesting the presence of SiO_2, NH_2 groups, CH_2, Cu_4O_3 and physisorbed H_2O. The optimum conditions for pH and adsorbent dosage were successfully evaluated for the adsorption process. The optimum pH at which the nanomaterial performed best was at pH 4. The optimum mass of the adsorbent that gave maximum adsorption performance was 20 mg. Kinetic studies revealed that the experimented data was in better correlation with pseudo-second-order kinetics. The outcome of this project would be of interest to textile industries looking for a cheap and effective way to treat textile wastewater.

KEYWORDS: *Adsorption, APTES, Methylene Blue, Nano adsorbent, Rice Husk, Silica, Sol-gel,*

1 INTRODUCTION

Pollution has become the inevitable by-product of the rapid spike in the industrial revolution. Out of many types of pollution that impact the environment, water pollution has become a serious concern in recent times (Owa, 2013). Water pollution is where the source of water is contaminated with undesirable inclusions and is left untreated to the extent that the water can no longer be used for general purposes (Halder & Islam, 2015). The main sources of water pollution are domestic wastewater, industrial wastewater, agricultural run-off, rainwater and sewage (Nag, 2018). In parts of Sri Lanka, urban areas have been polluted heavily with domestic sewage and industrial effluents. Rural areas suffer due to agricultural run-off (Berg,

ISSN 2961-5011 | https://doi.org/10.54389/VODW8508

2017). In certain parts of the dry zone, high fluoride and iron content have been reported. Overcrowded cities and areas encounter water-borne diseases due to poor drainage and sewage systems (Bandara, 2003). Industrial wastewater is one of the critical sources of water contamination. Wastewater from industrial outputs can severely affect the natural ecosystem by increasing salt and mineral content, changing the pH, increasing the ambient temperatures, depleting oxygen, etc (Maulin P, 2017). After agriculture, the textile dyeing industry is the most chemically intensive industry at the moment and has a major role to play in water pollution across the world. After agriculture, the textile dyeing industry is one of the most chemically intensive industries (Carmen & Daniela, 2012). Around 90-94% of water consumed by the textile industry is used as processing water. The common processes conducted include de-sizing, scouring, bleaching, mercerizing and dyeing processes. Effluents from these processes have become of alarming concern since they heavily contribute to the water pollution issues across the world. Around 2-20 % of textile dyes are discharged as effluents into different ecosystems (Carmen & Daniela, 2012).

The effluent from the textile industry negatively impacts the environment in many aspects irrespective of its model and area of disposal. Matter present in dyes causes issues such as bad appearance, prevention of sunlight penetration and oxygen into water, clogging pores in fields, corroding sewage pipes and providing a breeding ground for many types of bacteria and viruses.

There are various wastewater treatment methods established such as Granular Activated Carbon (GAC), Electro-Coagulation (EC), ultrasonic-treatment, Advanced Oxidation Process (AOP), Ozonation, Membrane Biological Reactor (MBR) and Sequencing Batch Reactor (SBR) (Bashir, 2016). However, most of these processes are quite expensive to set up and operate on an industrial scale (Carmen & Daniela, 2012). Adsorption is one of the widely explored types of purification processes. It is an efficient, effective and economical method for water purification (Gunathilaka et al., 2021). Many materials such as activated carbon, clay minerals, sawdust, zeolites, metal oxides, agriculture waste, and polymeric materials have been experimented with for adsorption of textile dyes from the effluent.

Activated carbon is commonly preferred due to its attractive features such as high surface area, porous structure, special surface reactivity, inertness, thermal stability and ability to be utilized over a range of pH. However, it has its limitations such as high cost, difficulty in removal of the exhausted carbon and inefficient performance of regenerated activated carbon (Zhuang et al., 2009).

Silica nanoparticles are another appealing option for the adsorption process due to their characteristics such as high surface area, ease of preparation, low-cost precursors, high compatibility for various surface modifications and acute toxicity. Moreover, silica nanoparticles can be obtained from rice husk which is a cheap precursor compared to other precursors to synthesize silica nanoparticles. Studies say that interaction with metals can help enhance the adsorption process in the removal of dye pollutants. Cu is a low-cost option that can be used to functionalize the surface of the silica nanoparticles (Makhlouf et al., 2008). Cu is well known for its ability to degrade organic pollutants such as dyes in a process known as the Fenton process (Fathima et al., 2008). Cu supported on mesoporous silica has shown excellent dye degradation performance (Sun et al., 2018). This research looks at synthesizing copper embedded surface-functionalized silica nanoparticles using rice husk as the precursor and the optimum condition for maximum performance of the nanomaterial.

2 METHODOLOGY

2.1 Materials

Sulfuric acid (98%, H_2SO_4), hydrochloric acid (37% HCl), sodium hydroxide, 2-propanol, 3-aminopropyl triethoxysilane (APTES), toluene, dichloromethane, and diethyl ether were purchased from Sigma-Aldrich (USA). Methylene Blue and copper (II) chloride dihydrate were purchased from Sisco Research Laboratories Pvt. Ltd. Maharastra (India). Rice husk was obtained from a paddy field in the Gampaha district.

2.2 Synthesis of silica nanoparticles

First, the rice husk was washed thoroughly. It was acid leached using 2M H_2SO_4 and 2M HCl and then calcined. Afterward, it was washed thoroughly and it was burnt in the muffle furnace. It was cooled down overnight and powdered nano-silica particles were obtained. Then 3M NaOH was added to the nano-silica particles. The solution was then heated and was stirred. Finally, it was filtered and the supernatant was obtained.

2.3 Integration of Copper onto silica nanoparticles

Initially, an APTES-Copper solution was prepared. APTES was added to a mixture of deionized water and propan-2-ol. Then Copper Chloride ($CuCl_2$) was added to deionized water. The $CuCl_2$ solution was added dropwise to the APTES solution while stirring. The amino group in APTES attaches to the Si-OH group of the nanomaterial thus acting as a linkage to functionalize Cu onto the nanomaterial. The supernatant was added dropwise to the APTES- Cu solution while stirring and a jelly-like solid residue was obtained. It was washed several times till neutral pH was obtained. The solid residue was allowed to dry. It was then crushed and ground into a fine powder. The fine powder was oven-dried and copper functionalized silica nanoparticles were obtained.

2.4 Performance of nanomaterial on anionic and cationic dyes

At first, the nanomaterial was tested to see which type of dye it adsorbs efficiently. Thus, Methylene Blue (MB), a cationic dye, and Methyl Orange (MO), an anionic dye, were chosen for the adsorption process. At first, 50 ml of 10 ppm of each dye solution were prepared. Then the nanomaterial was added to each solution. They were shaken using an orbital shaker. After diluting with deionized water, the absorbance values of each of the dye solutions were recorded every 5 minutes for 60 minutes.

2.5 Determination of optimum conditions

50 mg of the nanomaterial was added to a solution of 25 ml of 0.5 ppm MB. After shaking, it was diluted and the absorbance values were recorded. The steps were repeated in batch wise for concentrations, C (ppm) = 1.0, 1.5, 2.0, 2.5, 3.0 and 3.5. A calibration graph was plot and the molar absorbance coefficient was determined.

50 mg of nanomaterial was added to 50 ml of 10 ppm MB solution. The absorbance values were recorded by altering the pH batch wise by 2 for the range 2 to 12. The absorption uptake, q_t for a given pH was plotted against the time and the absorption uptake at equilibrium, q_e was determined.

50 ml of 10 ppm MB solution was transferred to a beaker, and its pH was altered to pH 4. The absorbance values were recorded by altering the mass of adsorbent dosage batch wise by 20 mg for the range 20 to 100. The q_t for a given mass was plotted against the time and the q_e was determined.

50 ml of 5 ppm MB solution was transferred to a beaker and its pH was altered to pH 4 and 20 mg of nanomaterial was added to the solution. The absorbance values were recorded every 5 minutes for 60 minutes. The steps were repeated for concentrations 10ppm and 15ppm batch wise. The q_t was plotted against the time and the q_e was determined.

2.6 Characterization of nanocomposite

The crystal structures present were determined via X-Ray Diffraction (XRD) using a Rigaku Ultima IV X-Ray Diffractometer (Cu Kα radiation, λ = 1.54060 Å) at the University of Sri Jayewardenepura. Chemical functional groups present in the sample were determined using ABB MB 3000 FT-IR spectrophotometer available at the Institute of Chemistry Ceylon.

3 RESULTS AND DISCUSSION

3.1 Characterization of nanomaterial

An FTIR was performed to determine the chemical functional groups and bonding present in the synthesized nanomaterial. Figure 1 illustrates the FTIR spectrum obtained for the sample. The values 800 cm^{-1} and 1042 cm^{-1} correspond to bending vibrations of Si - O - Si, Si - O symmetrical stretching and Si - O - Si asymmetrical stretching respectively (Biricik & Sarier, 2014). The presence of Cu-O stretching (600 cm^{-1}), Amino bending / in-plane bending of —O-H from residual H_2O (1645 cm^{-1}) and C—H stretching (2362 cm^{-1})) was also confirmed from the respective peaks from the spectrum (Singh et al., 2011).

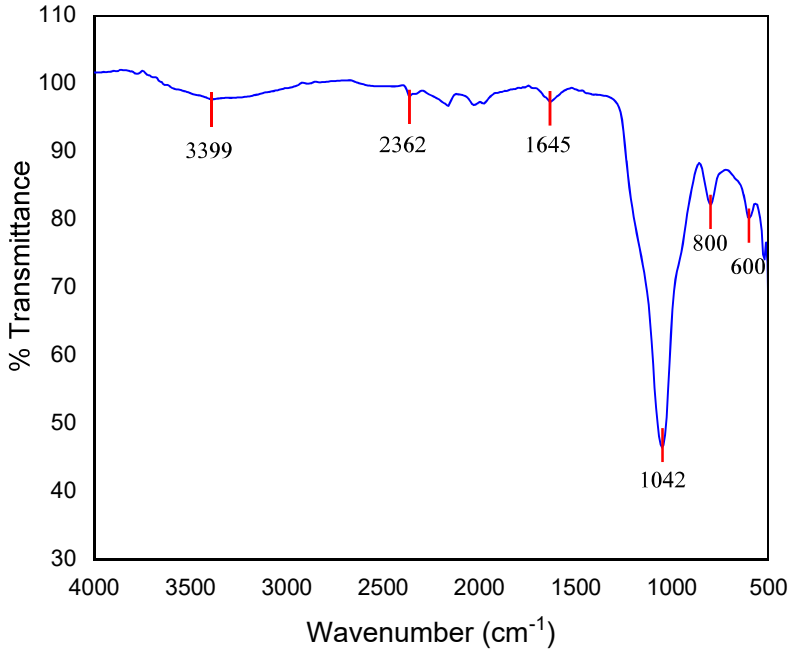

Figure 1. FTIR spectrum of Cu functionalized silica nanomaterial sample

Figure 2 shows the X-Ray Diffraction (XRD) pattern for the synthesized nanomaterial in the range of $2\theta = 5 - 80^{o}$ at a scan rate of 2. Distinct peaks were observed at $2\theta = 22.66^{o}$ and 35.57^{o} where they confirm the presence of Silicon Dioxide (SiO_2) and Copper Oxide (Cu_4O_3) respectively.

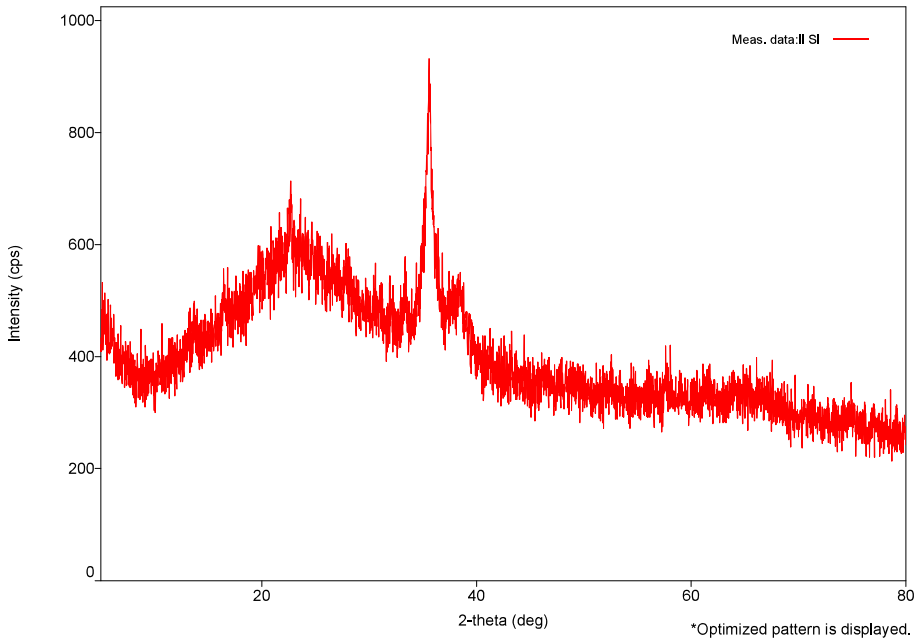

Figure 2. XRD pattern of Cu functionalized silica nanomaterial sample

3.2 Adsorption studies

At first, the nanomaterial was evaluated to see which type of dye it adsorbs efficiently. The nanomaterial was added to separate solutions containing MB and MO. The amount of dye removed from each solution was recorded and calculated to find the performance of the nanomaterial in both solutions. The performance of the nanomaterial on the type of dye was determined using the percentage removal method.

The percentage of dye removed was calculated using Equation (1):

$$\text{Percentage removal}(\%) = \frac{(A_0 - A_{60}) \text{x } 100}{A_0} \quad (1)$$

Where:

A_0 – initial absorbance

A_{60} – absorbance after 60 minutes

The amount of MB and MO removed was 62.15% and 2.20% respectively. Thus the nanomaterial was very good at adsorbing cationic dyes such as MB therefore the performance of the nanomaterial was evaluated using MB solution in the subsequent processes.

To evaluate the performance of the nanomaterial, the exact variations in concentration had to be recorded. The molar absorbent co-efficient of a given material is required to find the varying concentrations. Thus the molar absorbent co-efficient was determined using the help of a calibration plot shown in Figure 3, based on Beer-Lambert's Law. Beer-Lambert's law states there is a direct relationship between the concentration and absorbance of a given solution. Thus, the concentration of a solution can be determined if the absorbance can be measured. A procedure was conducted with varying concentrations of MB solutions (0.5 – 3.5 ppm) and the corresponding absorbance values were recorded.

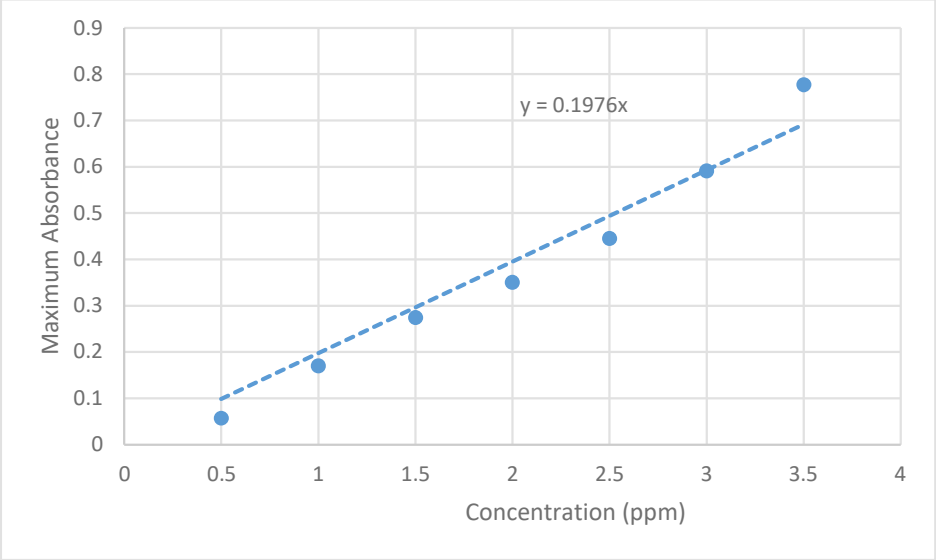

Figure 3. Calibration Plot of Methylene Blue solution

The molar absorption coefficient was determined as 0.1976 M^{-1} cm^{-1} from the gradient of the graph (Optical length was a constant value of 1 cm). The optimized conditions such as desirable pH, the mass of adsorbent were determined for the synthesized nanomaterial. The procedure was followed as mentioned in 2.5.

When taking absorbance reading, the MB solution was diluted with deionized water in a ratio of 1: 2. This was accounted for while calculating the concentration.
Thus, the concentration of the solution was calculated using Equation (2).

$$\text{Concentration, C} = \frac{\text{3 x Max. Absorbance}}{\text{Molar Absorption co-efficient}} \quad (2)$$

The concentration values were used to calculate adsorption uptake, q_t (mg g^{-1}), using Equation (3).

$$q_t = \frac{(C_0 - C_t)V}{m} \quad (3)$$

Where:

C_0 – initial concentration (ppm)

C_t – concentration at a given time, t (ppm)

V – the volume of adsorbate (MB) (dm^3)

m – the mass of adsorbent (mg)

The adsorption uptake at equilibrium, q_e (mg g^{-1}) tells us about the maximum adsorption uptake when the nanomaterial reaches saturation i.e. the material has reached its maximum capacity of adsorption. Higher the q_e value, the greater the adsorption of the substance. Figure 4 shows the effect of pH varying from 2- 12, on the adsorption uptake of MB solution by the nanomaterial. As the graph suggests, an increase in pH has increased the adsorption uptake until pH 4. The graph shows that the highest q_e has been recorded at pH 4 which is 7.84 mg g^{-1}. Further increase in pH did not influence the adsorption uptake thus resulting in lower q_e values (Karim et al., 2012).

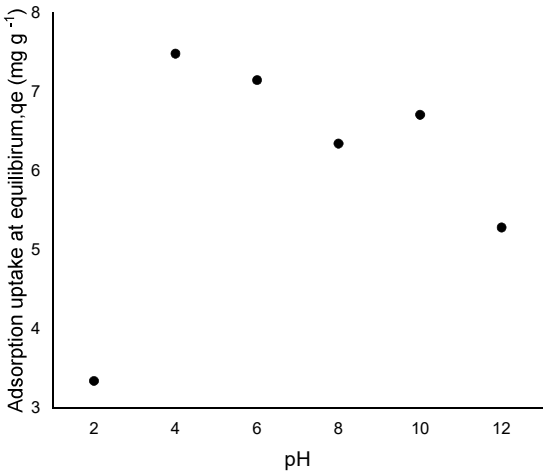

Figure 4. Effect of pH on adsorption uptake at equilibrium q_e

Figure 5 shows the effect of the mass of the adsorbent on the adsorption uptake at equilibrium. The effect was studied in the mass range of 20 - 100 mg and MB concentration of 10 ppm. The mass of the adsorbent determines the amount of surface area available for the adsorption process. As the graph depicts, the increase in the mass of the adsorbent has decreased the adsorption uptake. The highest adsorption uptake at equilibrium was 9.982 mg g^{-1} and was recorded at the lowest amount of adsorbent which is 20 mg. This is because a small amount of adsorbent means, a larger overall surface area is exposed to the MB solution for adsorption to take place, compared to the other masses. Thus, more MB cations would have been adsorbed resulting in the highest q_e value at 20 mg (Karim et al., 2012).

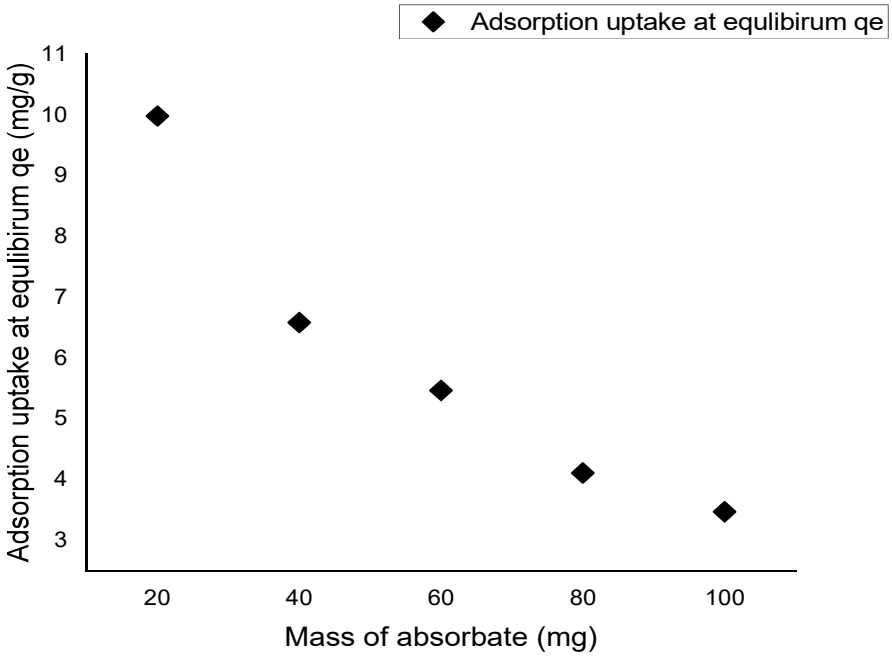

Figure 5. Effect of the mass of adsorbent on adsorption uptake at equilibrium, q_e

Once the optimum pH and the mass of the adsorbent were determined, the performance of the nanomaterial was tested. MB solutions of varying concentrations from 5 – 15 ppm have experimented with 20 mg of the nanomaterial at pH 4.

Figure 6 shows the effect of initial concentration on the performance of the nanomaterial. The adsorption uptake increases quickly until 20 minutes. From 20 minutes onwards, in both 5 and 10 ppm, the qt values gradually decreased to reach equilibrium. However, in 15 ppm, the adsorption activity did not seem to reach equilibrium significantly. It is visible that when the initial concentration of MB is increased, the adsorption uptake has also increased. This is because of the larger concentration gradient created by the higher concentration that serves as a driving force for the adsorption process. 15 ppm seems to show the highest adsorption with a qe value of 11.01 mg g^{-1}. The short time taken to reach close to equilibrium indicates the affinity of the dye molecules towards the nanomaterial resulting in effective adsorption (Karim et al., 2012).

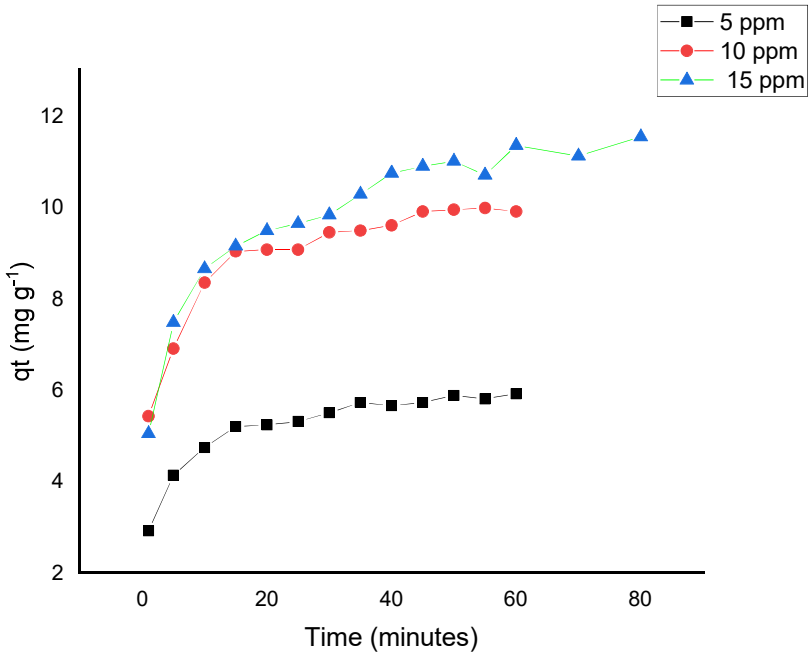

Figure 6. Performance of nanomaterial on different initial MB concentrations

3.3 Kinetics Model

Adsorption kinetics is an important concept to study the adsorption uptake rate and understand the nature of the adsorption process. To evaluate the performance of the nanomaterial on the adsorption process, the experimental data were fit into 2 conventional kinetic models and were interpreted.

These kinetic models are;

Lagergren Pseudo First Order: $$\ln(q_e - q_t) = lnq_e - k_1 t \quad (4)$$

Ho Pseudo Second Order: $$\frac{t}{q_t} = \frac{1}{k_2 q_e^2} + \frac{t}{q_e} \quad (5)$$

Where;

q_e – adsorption uptake at equilibrium (mg g^{-1})

q_t – adsorption uptake at time,t (mg g^{-1})

k_1 – rate constant for pseudo first order (min^{-1})

k_2 – rate constant for pseudo second order (g mg^{-1} min^{-1})

t – Time (min)

Since the equations are linear expressions, k_1 can be determined from the gradient of a pseudo-first-order graph and k_2 can be calculated using the gradient and intercept of a pseudo-second-order graph (Dashamiri et al., 2017). The validity of a certain model towards the experimental study is determined by the correlation coefficient and how close the theoretical and experimental adsorption uptake match. This is indicated by the R^2 value. The adsorption experimented were fitted into both pseudo-first-order and pseudo-second-order models. Table 1 summarizes the kinetic information obtained for both Pseudo first and second order.

Table 1. Co-efficient of pseudo-first- and second-order adsorption kinetic models

Initial Concentration (ppm)	Pseudo First Order			Pseudo Second Order		
	qe (mg g^{-1})	k_1 (min^{-1})	R^2	qe (mg g-1)	k_2(g mg^{-1} min^{-1})	R^2
5	3.0446	0.0721	0.9203	6.0919	0.0640	0.9986
10	5.6277	0.0877	0.8701	10.2774	0.0432	0.9988
15	7.3472	0.0794	0.9166	11.8259	0.0209	0.9965

The graphs obtained for pseudo-first order and pseudo-second-order are illustrated in Figure 7.

a) b)

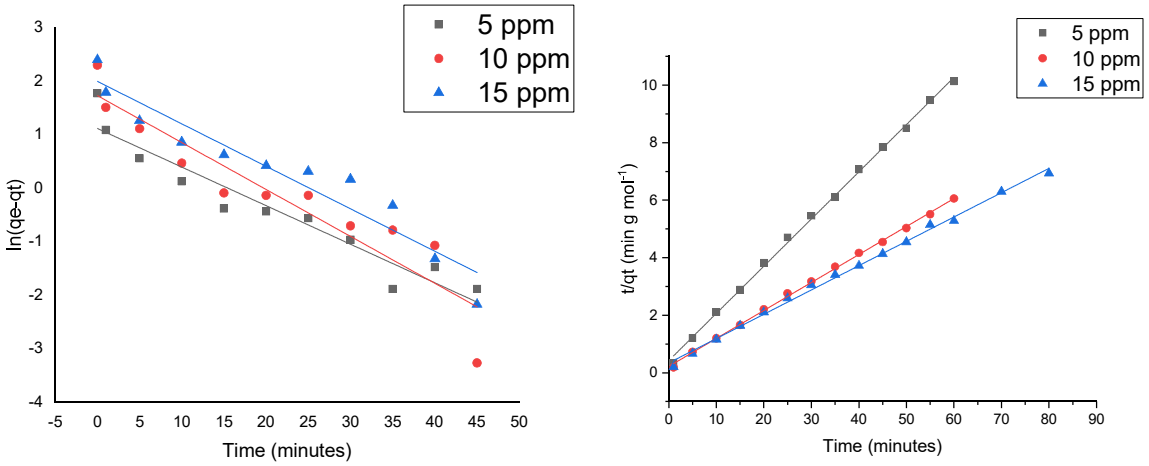

Figure 7. a) Pseudo-first order and b) pseudo-second-order kinetics model for MB adsorption onto nanomaterial

It is clear from the data in Table 2 and Figure 7 that pseudo-second-order has R^2 values much closer to 1 than pseudo-first-order. This indicates that the experimental data closely adhered to pseudo-second-order kinetics (Hu et al., 2014) (Dahri et al., 2015).

4 CONCLUSION

This research aimed at synthesizing silica nanoparticles from rice husk which is a relatively cheap precursor in the Sri Lankan context. The silica was surface-functionalized using Cu, another cheap element, to enhance its adsorption performance to remove organic dyes from textile effluent. The dye used in this research was methylene blue. The XRD results confirmed the presence of major compounds such as silicon dioxide and copper oxide as predicted. The FTIR confirmed the presence of expected chemical bonds such as Si–O stretching, C–H stretching, Cu–O stretching and O–H bending. The optimum conditions for the best performance of the nanomaterial have been experimented with. The optimum pH at which the nanomaterial performed best was at pH 4. The optimum mass of the adsorbent that gave maximum adsorption performance was 20 mg. Once the optimum parameters were determined, the nanomaterial was exposed to varying methylene blue concentrations of 5ppm, 10ppm and 15ppm. Kinetic studies revealed that the experimented data was in better correlation with pseudo-second-order kinetics.

5 ACKNOWLEDGEMENT

The authors acknowledge the Sri Lanka Institute of Information Technology and the World Bank Project for providing financial support, laboratory facilities and material resources. We also extend our gratitude to Prof. Nilwala Kottegoda for her support in obtaining the X-Ray Diffraction test results and Mrs.Himasha Gunathilaka for her technical support during the initial phases of the project.

6 REFERENCES

Owa, F. (2013). Water Pollution: Sources, Effects, Control and Management. Mediterranean Journal of Social Sciences. https://doi.org/10.5901/mjss.2013.v4n8p65

Halder, J., & Islam, N. (2015). Water Pollution and its Impact on the Human Health. Journal of Environment and Human, 2(1), 36–46. https://doi.org/10.15764/eh.2015.01005

Nag O.S. (2018, October 9). *World Atlas*. World Atlas. Retrieved September 1, 2020, from https://www.worldatlas.com/articles/how-many-types-of-pollution-are-there.html

Berg, S. (2017, April 24). *Types of Pollutants*. SCIENCING. Retrieved September 1, 2020, from https://sciencing.com/types-pollutants-5270696.html

Bandara, N. (2003). Water and wastewater related issues in Sri Lanka. *Water Science & Technology*, *47*(12), 305–312.

Maulin P, S. (2017). Waste Water Pollution. Journal of Applied Biotechnology & Bioengineering, 3(1). https://doi.org/10.15406/jabb.2017.03.00054

Carmen, Z., & Daniela, S. (2012). *Textile Organic Dyes – Characteristics, Polluting Effects and Separation/Elimination Procedures from Industrial Effluents*. InTech.

Zhuang, X., Wan, Y., Feng, C., Shen, Y., & Zhao, D. (2009). Highly Efficient Adsorption of Bulky Dye Molecules in Wastewater on Ordered Mesoporous Carbons. Chemistry of Materials, 21(4), 706–716. https://doi.org/10.1021/cm8028577

Bashir, N. (2016, December 3). *Waste water treatment ppt*. Slideshare. Retrieved September 12, 2020, from https://www.slideshare.net/NusratBashir3/waste-water-treatment-ppt

Gunathilaka, H., Thambiliyagodage, C., Usgodaarchchi, L., & Angappan, S. (2021). Effect of surfactants on morphology and textural parameters of silica nanoparticles derived from paddy husk and their efficient removal of methylene blue. International Conference on Innovations in Energy Engineering & Cleaner Production IEECP21, 21. https://doi.org/10.6084/m9.figshare.14904873

K. (2013, April 11). *Waste water treatment*. Slideshare. Retrieved September 12, 2020, from https://www.slideshare.net/kumar_vic/waste-water-treatment-18653689

Makhlouf, C., Baouab, M. H. V., & Roudesli, S. (2008). Use of the [Copper(II)/MAA-nylon] Complex for the Adsorption of Residual Acid Dyes. *Adsorption Science & Technology*, *26*(6), 433–447. https://doi.org/10.1260/0263-6174.26.6.433

Fathima, N. N., Aravindhan, R., Rao, J. R., & Nair, B. U. (2008). Dyehouse wastewater treatment through advanced oxidation process using Cu-exchanged Y zeolite: A heterogeneous catalytic approach. *Chemosphere*, *70*(6), 1146–1151. https://doi.org/10.1016/j.chemosphere.2007.07.033

Sun, B., Li, H., Li, X., Liu, X., Zhang, C., Xu, H., & Zhao, X. S. (2018). Degradation of Organic Dyes over Fenton-Like Cu2O–Cu/C Catalysts. *Industrial & Engineering Chemistry Research*, *57*(42), 14011–14021. https://doi.org/10.1021/acs.iecr.8b02697

Biricik, H., & Sarier, N. (2014). Comparative study of the characteristics of nano-silica -, silica fume - and fly ash - incorporated cement mortars. *Materials Research*, *17*(3), 570–582. https://doi.org/10.1590/s1516-14392014005000054

Singh, L. P., Agarwal, S. K., Bhattacharyya, S. K., Sharma, U., & Ahalawat, S. (2011). Preparation of Silica Nanoparticles and its Beneficial Role in Cementitious Materials. *Nanomaterials and Nanotechnology*, *1*, 9. https://doi.org/10.5772/50950

Karim, A., Jalil, A., Triwahyono, S., Sidik, S., Kamarudin, N., Jusoh, R., Jusoh, N., & Hameed, B. (2012). Amino modified mesostructured silica nanoparticles for efficient adsorption of methylene blue. *Journal of Colloid and Interface Science*, *386*(1), 307–314. https://doi.org/10.1016/j.jcis.2012.07.043

Dashamiri, S., Ghaedi, M., Asfaram, A., Zare, F., & Wang, S. (2017). Multi-response optimization of ultrasound assisted competitive adsorption of dyes onto Cu (OH)2-nanoparticle loaded activated carbon: Central composite design. *Ultrasonics Sonochemistry*, *34*, 343–353. https://doi.org/10.1016/j.ultsonch.2016.06.007

Hu, J., Yu, H., Dai, W., Yan, X., Hu, X., & Huang, H. (2014). Enhanced adsorptive removal of hazardous anionic dye “congo red” by a Ni/Cu mixed-component metal–organic porous material. *RSC Adv.*, *4*(66), 35124–35130. https://doi.org/10.1039/c4ra05772d

Dahri, M. K., Kooh, M. R. R., & Lim, L. B. (2015). Application of Casuarina equisetifolia needle for the removal of methylene blue and malachite green dyes from aqueous solution. *Alexandria Engineering Journal*, *54*(4), 1253–1263. https://doi.org/10.1016/j.aej.2015.07.005